Eur. Phys. J. C (2025) 85:450
https://doi.org/10.1140/epjc/s10052-025-14146-5

THE EUROPEAN PHYSICAL JOURNAL C

Regular Article - Theoretical Physics

Charged compact star models in extended symmetric teleparallel gravity and influence of charge and coupling parameters on the star configuration

S. K. Maurya[1,a], **Fadhila Al Khayari**[1,b], **G. Mustafa**[2,c], **Baiju Dayanandan**[3,d], **Phongpichit Channuie**[4,5,e], **Farruh Atamurotov**[6,7,f]

[1] Department of Mathematical and Physical Sciences, College of Arts and Sciences, University of Nizwa, 616 Nizwa, Sultanate of Oman
[2] Department of Physics, Zhejiang Normal University, Jinhua 321004, People's Republic of China
[3] Natural and Medical Sciences Research Center, University of Nizwa, 616 Nizwa, Sultanate of Oman
[4] School of Science, Walailak University, Nakhon Si Thammarat 80160, Thailand
[5] College of Graduate Studies, Walailak University, Nakhon Si Thammarat 80160, Thailand
[6] New Uzbekistan University, Movarounnahr Street 1, 100000 Tashkent, Uzbekistan
[7] Urgench State University, Kh. Alimdjan str. 14, Urgench 220100, Uzbekistan

Received: 11 February 2025 / Accepted: 30 March 2025

Abstract In this paper, the modified field equations in the context of Extended symmetric teleparallel gravity theory are considered for isotropic and charged compact stellar configuration. In order to obtain an exact solution to the modified field equations, we find an isotropy condition of the charge matter distribution in extended symmetric teleparallel gravity. After that, a regular and well-behaved electric field and a metric potential ansatz are used to solve this isotropy condition. Based on this specific choice, the obtained exact solution hence represents the characteristics and features of the stellar system such as charge, density, and pressure which are shown to be physically valid. The adiabatic stability condition as well as the influence of non-minimal coupling of non-metricity scalar and trace of energy–momentum tensor on stellar configuration have been performed. The present gravitational model investigates some known observed compact stars, viz. PSR J074 +6620, PSR J2215+5135, PSR J1748-2446ao, and GW190814 successfully by exploring mass-radius relationship enabling the model parameters. The present model describing the physical star with isotropic fluid and density of the order of 10^{14} g/cm^3 is unable to account for the radii of the star falling in the mass gap region with respect to the parameters representing non-metricity and electric field. An increase in a model parameter representing the matter part in the non-minimal coupling justifies the existence of the compact stars in mass gap regions like GW190814 with predicted radii in the range [10.87, 12.49] km in the present isotropic charged stellar model in extended symmetric teleparallel gravity.

[a] e-mail: sunil@unizwa.edu.om
[b] e-mail: fadhila@unizwa.edu.om
[c] e-mail: gmustafa3828@gmail.com
[d] e-mail: baiju@unizwa.edu.om
[e] e-mail: phongpichit.ch@mail.wu.ac.th (corresponding author)
[f] e-mail: atamurotov@yahoo.com

Contents

Published online: 24 April 2025

1 Introduction

Recent observational evidence regarding the accelerated expansion of the Universe enriches our understanding of the formation of the enigmatic Universe. In particular, different astrophysical events associated with the origin and evolution of large-scale structures have drawn significant attention among scientists in the field of astrophysics and astronomy. Subsequently, the study of various astrophysical objects become a fascinating area of research. In this regard, after the exhaustion of thermonuclear fuel gravitational collapse of self-gravitating bodies depending on the initial mass of the main sequence star produces different types of compact objects (COs) such as white dwarfs, neutron stars, and black holes. The stability of these COs is attained when degeneracy pressure due to neutrons or electrons balances the inward gravitational pull and resists further gravitational collapse. The properties of the compact structure of COs can be explored by obtaining an exact and analytic solution of nonlinear differential equations in the context of a gravitational theory. Schwarzschild [1] obtained the vacuum solution of the non-linear field equations for COs in the background of general relativity (GR).

GR is seen to be competent with the experimental tests that are based on the probes of weak-field gravity at intermediate energy scales so far along with the exception of astronomical observations of binary pulsar. Nevertheless, some rising theoretical and experimental issues suggest certain modifications of GR at small and large energy scales. From a theoretical perspective, power-counting arguments imply that GR being a purely classical theory can not be renormalizable by methods in the standard quantum field theory. With inclusion of quadratic curvature terms representing high-energy corrections to the Einstein–Hilbert action [2], GR can be renormalizable under strong-field modifications. Besides the singularity problem in GR as indicated by Hawking and Penrose [3] can be resolved by high-curvature corrections. String theory and loop quantum gravity are such theories that specify the nature of required modifications of GR at high energies.

From an observational perspective, detections and measurements in cosmology are generally comprehended to support the possible existence of dark matter (DM) and dark energy as a form of a nonzero cosmological constant. As a consequence, some serious theoretical issues such as the cosmological constant problem and the coincidence problem concern researchers. Further, a dynamical solution in connection to the cosmological constant problem can not be obtained in the context of GR [4] which indicates low energy corrections to GR are needed. This has been a critical issue for the scientists to include corrections in GR at low as well as high energies in such a way that the modifications are in alignment with GR at intermediate-energy scales. The modification of GR can be designed in such ways that it is in concurrence with the recent observations. Experimental explorations beyond GR theory become a thriving field of research.

Lovelock's theorem [5] simply implies that GR can be considered as the unique gravitational theory subject to definite assumptions. By circumventing any of the assumptions in Lovelock's theorem one may find different ways to find different modified theories of gravity. Including additional degrees of freedom as a form of extra fields coupled to gravity is the simplest way to evade Lovelock's theorem and give rise to various possibilities for the modifications of GR. For instance, the theory of scalar–tensor gravity [6] incorporates additional scalar degrees of freedom via non-minimal coupling to gravity. Horndeski gravity [7] having a second-order field equation appears to be the most general form of scalar-tensor gravity. In order to explain the cosmic explanation infrared corrections to GR have been proposed as a form of $f(\mathcal{R})$ gravity theory [8] where $\mathcal{R}$ is scalar curvature. The Lagrangian in the Einstein–Hilbert action is modified or extended by incorporating a function of the curvature scalar. It has been a difficult task to develop $f(\mathcal{R})$ theories [9–11] in such a manner that it could generate different nature at cosmological and remain viable observationally at small scales. Subsequently, higher-curvature corrections rather than $f(\mathcal{R})$ models have been proposed to be included in actions. The construction of such complicated action can be developed by incorporating the Gauss–Bonnet combination $\mathbb{G}$ [12,13] or arbitrary functions $f(\mathbb{G})$ [14,15] in curvature gravity.

The teleparallel equivalent of general relativity (TEGR) is another form of gravitational modification. The formulation of gravity on the basis of torsion ($\mathbb{T}$), namely $f(\mathbb{T})$ gravity [16–18] is one such modification. The Lagrangian in $f(\mathbb{T})$ gravity includes a function of the torsion motivated by the curvature-based gravity like $f(\mathcal{R})$ gravity. In the TEGR approach, the curvature scalar being expressed to a general connection is articulated as Levi–Civita connection with added torsion tensor terms. After applying the teleparallelism condition $\mathcal{R}_{abcd} = 0$ we get the curvature scalar as the sum of a torsion scalar and a total derivative. So, gravity is related to torsion by the condition of teleparallelism where the gravitational interaction does not arise from the geometric description but as a form of force. One of the key benefits of adopting $f(\mathbb{T})$ gravity theory is that the field equations are of second order in comparison with the $f(\mathcal{R})$ gravity where the field equations are of fourth order.

With the same approach of teleparallelism one can acquire the teleparallel equivalent of the $\mathbb{G}$ as $\mathbb{T}_{\mathbb{G}}$ and combine it with $\mathbb{T}$ to develop possible extensions such as the $f(\mathbb{T}, \mathbb{T}_{\mathbb{G}})$ modified gravity [19]. Another possible extension of $f(\mathbb{T})$ gravity can be obtained as $f(\mathbb{T}, T)$ gravity [20] by a general coupling between $\mathbb{T}$ being geometric part of the action and the trace of the matter energy–momentum tensor T being non-geometric part of the action. With similar technique, when the matter

Lagrangian $\mathcal{L}_m$ is combined with functions of the $\mathcal{R}$ we get extended the theory as $f(\mathcal{R}, \mathcal{L}_m)$ gravity [21–23]. Further, T can be coupled with $\mathcal{R}$ to build in $f(\mathcal{R}, T)$ gravity theory [24–26]. Recently, another modified theory $f(\mathcal{R}, \mathbb{T})$ [27–29] with Lagrangian having Ricci scalar as well as Torsion scalar attracts significant attention among the theorists.

One of the properties related to vectors known as non-metricity can be incorporated into the Lagrangian of the modified theories of gravity. In general, the metric represents the idea of distance from which we can obtain the definition of the non-metricity tensor ($Q_{\alpha\mu\eta}$). Physically, $Q_{\alpha\mu\eta}$ implies the change in length of a vector being parallel transported along a curve under some specific connection $\Gamma_{\alpha\mu\eta}$. Further, non-metricity can determine the variation in angles between two parallel transported vectors. The description of gravity in a zero curvature and torsionless spacetime with non-vanishing non-metricity tensor forms the symmetric teleparallel equivalent of general relativity (STEGR). If we incorporate arbitrary function f of non-metricity scalar in Lagrangian we get $f(Q)$ gravity [30,31]. The application of different $f(Q)$ gravity models in the field of cosmology can be found in literature investigating the late-time Universe [32–34], construction of large scale structures [35], study of relativistic versions of MOND [36,37], questions pertaining to bouncing cosmologies [38–40], and quantum cosmology [41,42]. In connection to copact stars, Maurya et al. [43] recently used a quadratic equation of state alongside a linear formulation for $f(Q)$ to investigate compact objects inside the MGD framework. The most reliable model, which encompasses a broad range of stars, particularly compact objects with masses predicted by GW190814, is the one that includes a superposition of linear and quadratic contributions from stellar density. Bhar et al. studied charged compact objects with anisotropic fluid in the interior to examine the impact of the quadratic factor in $f(Q) = Q + aQ^2$, which reverts to classical GR when $a = 0$ [44]. They showed that the models they developed were responsive to the equation of state parameter, metricity, charge, and the bag constant. Furthermore, they observed that the quadratic contribution from $f(Q)$ leads to a reduction in density, radial pressure, electric field, and sound velocity. The originality of their research is in the capacity to enhance the degree of anisotropy via the quadratic term in $f(Q)$, without resorting to gravitational decoupling or other unconventional scalar fields or matter configurations, including dark energy. For a recent examination of $f(Q)$ gravity, we direct the reader to [45] for more information. Moreover, Alwan et al. [46] have investigated the neutron star models in generalized form $f(Q)$ functions as (i) $f(Q) = Q + \alpha Q^2$, (ii) $f(Q) = Q + \alpha e^{\beta Q}$, and (iii) $f(Q) = Q + \alpha \ln(1 - \beta Q)$. They solved the TOV equation numerically using a realistic equation of state to find the solution of neutron star models.

Studies on the successful applications of $f(\mathcal{R}, T)$ gravity in the field of astrophysics and cosmology can be found in literature [47–71]. So, we are motivated to employ an extension of $f(Q)$ gravity known as $f(Q, T)$ gravity which is obtained via non-minimal coupling between Q and T in the present study,. In this case, an arbitrary function of both Q and T is incorporated in the Lagrangian to build the geometric action which can be varied with respect to the metric tensor in order to derive the gravitational field equations describing geometry-matter coupling. The covariant derivative of the gravitational field equations in $f(Q, T)$ gravity leads to non zero divergence of the energy–momentum tensor which is a key feature of the present non-minimal gravitational interaction. The non conservation of energy–momentum tensor physically infers necessary variations in the thermodynamical properties of the Universe as indicated in the $f(\mathcal{R}, T)$ theory [72]. Further, an additional force due to deviation of test particles from geodesic path to non-geodesic path exists in the current approach of gravitational theory. A recent study [73] establishes the theoretical consistency of $f(Q, T)$ gravity theory in connection to different cosmological aspects such as cosmic expansion and dark energy.

A general perspective [74,75] of physical unattainability of the charged configuration of astrophysical compact objects with strong electric field had been confronted by several studies [75–78]. The possibility of attaining huge amounts of charge by compact objects in the accreting gravitational systems or in the process of gravitational collapse becomes the indispensable area of research [79,80]. The bulk characteristics of compact star can be influenced by the presence of strong electric field in the gravitational configuration [81–84]. Some studies [85,86] analyzed the influence of electromagnetic fields on the physical characteristics of compact objects such as maximum mass, luminosities and redshift. Further, the effect of the presence of electromagnetic field on the configuration of quark stars had been examined in research works [87,88]. Considering isotropic pressures and a well-behaved functional form of the electric field a study [89] obtained physical solutions to the Einstein-Maxwell system that seems to follow a barotropic equation of state and corresponds to the Finch and Skea model [90].

We want to develop a new analytical solution describing well-behaved physical properties of relativistic isotropic and charged stellar configurations. In this regard, we assume the linear form of the f function of Q and T in addition to a metric potential ansatz [97] and a well-behaved electric field in the framework of $f(Q, T)$ gravity. The investigations in the paper are organized as follows: A brief review of $f(Q, T)$ gravitational theory is given in Sect. 2. Then an exact solution to the modified field equations considering metric potential ansatz and electric field is provided in Sect. 3. We determine unknown constants using the boundary condition in Sect. 4. The physical features of the stellar system such as charge, density, and pressure are explored in Sect. 5. Further analysis of the equation of state is given on the basis of sound speed

in Sect. 6. The stability of the stellar system is examined by adiabatic condition in Sect. 7. Importantly, the investigation of mass-radius relation in connection to observational constraints is presented in Sect. 8. In Sect. 9 we make some final comments.

2 A summary of extended symmetric teleparallel gravity

We will express action in context of extended symmetric teleparallel gravity i.e. $f(Q,T)$, in general and integral form as [91],

$$S=\int\sqrt{-g}\Big[\frac{1}{2}f(Q,T)+\mathcal{L}_M+\mathcal{L}_e\Big]d^4x. \tag{1}$$

where the Lagrangian density is presented by $\mathcal{L}_M$ and $\mathcal{L}_e$ in connection to the energy–momentum tensor expressed as $T_{\mu\eta}$ and electromagnetic field tensor $\mathcal{E}_{\mu\eta}$, respectively. Additionally, g is the determinant of the metric tensor and relativistic units have been taken as: $8\pi G=c=1$)

With regard to the affine connection $\Gamma^{\delta}{}_{\kappa\mu}$ the non-metricity tensor can be expressed as,

$$Q_{\kappa\mu\eta}\equiv\nabla_\kappa g_{\mu\eta}=\partial_\kappa\, g_{\mu\eta}-\Gamma^{\delta}{}_{\kappa\mu}\, g_{\delta\eta}-\Gamma^{\delta}{}_{\kappa\eta}\, g_{\mu\delta}, \tag{2}$$

where we have

$$\Gamma^{\delta}{}_{\kappa\mu}=\left\{\begin{matrix}\delta\\ \kappa\mu\end{matrix}\right\}+K^{\delta}{}_{\kappa\mu}+L^{\delta}{}_{\kappa\mu}. \tag{3}$$

Here $\left\{\begin{matrix}\delta\\ \kappa\mu\end{matrix}\right\}$ is Levi–Civita connection. Again $L^{\delta}{}_{\kappa\mu}$ is contorsion tensor and $K^{\delta}{}_{\kappa\mu}$ is termed as disformation tensor. These quantities are expressed mathematically as,

$$\left\{\begin{matrix}\delta\\ \kappa\mu\end{matrix}\right\}=\frac{1}{2}\,g^{\delta\varphi}\left(\partial_\kappa g_{\varphi\mu}+\partial_\mu g_{\delta\eta}-\partial_\delta g_{\kappa\mu}\right), \tag{4}$$

$$K^{\delta}{}_{\kappa\mu}=\frac{1}{2}T^{\delta}{}_{\kappa\mu}+T_{(\kappa}{}^{\delta}{}_{\mu)}, \tag{5}$$

$$L^{\delta}{}_{\kappa\mu}=\frac{1}{2}Q^{\delta}{}_{\kappa\,\mu}-Q_{(\kappa}{}^{\delta}{}_{\mu)}, \tag{6}$$

where torsion tensor is written as $T^{\delta}{}_{\kappa\mu}$.

The superpotential $P^{\varphi}{}_{\mu\eta}$ regarded to be one of the important quantities in the framework of STEGR is presented as,

$$P^{\varphi}{}_{\mu\eta}=-\frac{1}{2}L^{\varphi}{}_{\mu\eta}+\frac{1}{4}\left(Q^{\varphi}-\tilde{Q}^{\varphi}\right)g_{\mu\eta}-\frac{1}{4}\delta^{\varphi}{}_{(\mu}\,Q_{\eta)}, \tag{7}$$

where

$$Q_\varphi=Q_\varphi{}^{\mu}{}_{\mu},\quad \tilde{Q}_\varphi=Q^{\mu}{}_{\varphi\mu},$$

are the trace of the non-metricity tensor.

Eventually, we can define the non-metricity scalar as,

$$Q=-Q_{\varphi\mu\eta}P^{\varphi\mu\eta}. \tag{8}$$

The variation of the action (1) with regard to the inverse of metric tensor $g^{\mu\eta}$ provides the gravitational field equations associated to the $f(Q,T)$ as

$$\begin{aligned}&\frac{2}{\sqrt{-g}}\nabla_\varphi\left(f_Q\sqrt{-g}\,P^{\varphi}{}_{\mu\eta}\right)\\&+f_Q\left(P_{\mu\varphi\kappa}\,Q_\eta{}^{\varphi\kappa}-2Q^{\varphi\kappa}{}_{\mu}\,P_{\varphi\kappa\eta}\right)\\&+\frac{1}{2}f\,g_{\mu\eta}=-(T_{\mu\eta}+\mathcal{E}_{\mu\eta})+f_T\left(T_{\mu\eta}+\Phi_{\mu\eta}\right).\end{aligned} \tag{9}$$

Where, $f_Q=\frac{\partial f(Q,T)}{\partial Q}$, $f_T=\frac{\partial f(Q,T)}{\partial T}$.

The energy momentum tensor termed as $T_{\mu\eta}$ can be expressed as

$$T_{\mu\eta}=-\frac{2}{\sqrt{-g}}\frac{\delta(\sqrt{-g}\mathcal{L}_m)}{\delta g^{\mu\eta}}, \tag{10}$$

$$\mathcal{E}_{\mu\eta}=\frac{2}{\sqrt{-g}}\frac{\delta\left(\sqrt{-g}\,\mathcal{L}_e\right)}{\delta g^{\mu\eta}}. \tag{11}$$

Moreover, another quantity known as the hyper-momentum tensor given by $\Phi_{\mu\eta}=g^{\varphi\beta}\frac{\delta T_{\varphi\beta}}{\delta g^{\mu\eta}}$ is present in the Eq. (9).

An extra constraint can be inferred from Eq. (1) as,

$$\nabla_\mu\nabla_\eta(\sqrt{-g}f_Q P^{\varphi}{}_{\mu\eta})=0. \tag{12}$$

The curvature-free as well as torsion-free constraints [92] lead to the affine connection given by

$$\Gamma^{\varphi}{}_{\mu\eta}=\left(\frac{\partial x^\varphi}{\partial\xi^\alpha}\right)\partial_\mu\partial_\eta\xi^\alpha. \tag{13}$$

With the choice of co-incident gauge, we obtained $\Gamma^{\varphi}{}_{\mu\eta}=0$. Hence, we get the non-metricity equation as

$$Q_{\kappa\mu\eta}\equiv\nabla_\kappa g_{\mu\eta}=\partial_\kappa\, g_{\mu\eta}, \tag{14}$$

which is the function of the metric only. As a consequence, the computation technique is simplified.

It is worth mentioning that diffeomorphism invariance is not anymore maintained in the action excluding the case with the STGR [93]. The covariant formulation of $f(Q)$ gravity can resolve such obstacle related to the diffeomorphism invariance. Considering the inertial form of the affine connection given in Eq. (13) the covariant formulation by the affine connection can be employed without the effect of gravity. [94].

The electromagnetic energy–momentum tensor $E_{\mu\eta}$ can be written mathematically as,

$$E_{\mu\eta}=2\left(F_{\mu k}F_{\eta k}-\frac{1}{4}g_{\mu\eta}F_{kl}F^{kl}\right),$$

where

$$F_{\mu\eta}=\mathcal{A}_{\mu,\eta}-\mathcal{A}_{\eta,\mu}.$$

Here $\mathcal{A}_\mu$ is the electromagnetic four potential.

Furthermore, we can express the electromagnetic field tensor as,

$$F_{\mu\eta,k} + F_{k\mu,\eta} + F_{\eta k,\mu} = 0, \tag{15}$$

$$\left(\sqrt{-g}F^{\mu\eta}\right)_{,\eta} = \frac{1}{2}\sqrt{-g}J^{\mu}, \tag{16}$$

where J^{μ} is the four current density is represented.

The only nonzero component of J^{μ} is J^0 being oriented along the radial direction r on the account of spherically symmetric and static fluid configuration. With the same considerations, we get the only non vanishing component of electromagnetic field tensor as F_{01}. Further, the antisymmetry indicates that the condition $F_{01} = -F_{10}$ and Eq. (16) are satisfied. Hence the expression of the electric field can presented from Eq. (16) as:

$$\mathcal{E}(r) = \frac{1}{2r^2}\int_0^r x^2\,\sigma(x)\sqrt{g_{rr}}\,dx = \frac{q(r)}{r^2}, \tag{17}$$

where σ and $q(r)$ signify the charge density and total charge respectively.

3 Modified gravitational field equation in $f(Q,T)$ gravity

In the present investigation, spherically symmetric and static metric is assumed to describe the interior of the compact object,

$$ds^2 = -\mathcal{F}_0^2(r)dt^2 + \mathcal{H}_0^2(r)dr^2 + r^2(d\theta^2 + \sin^2\theta\, d\phi^2), \tag{18}$$

where $\mathcal{F}_0(r)$ and $\mathcal{H}_0(r)$ are the static metric potentials.

We have characterize the stellar dense matter with a perfect fluid configuration along with the components of the energy–momentum tensor expressed as $(-\rho, P, P, P)$. Notably, the density of the isotropic matter configuration is ρ and the isotropic pressure is depicted as P. Moreover, we have made a choice for the matter Lagrangian as $L_m = P$ based on the studies [95,96]. Therefore, we have the components of $\Phi_{\mu\eta}$ as $\Phi_{\mu\eta} = g_{\mu\eta}P - 2T_{\mu\eta}$.

Now, the non-metricity scalar can be expressed in terms of metric potentials as

$$Q = -\frac{2(2r\mathcal{F}_0'(r) + \mathcal{F}_0)}{r^2\,\mathcal{F}_0\,\mathcal{H}_0^2}. \tag{19}$$

In the present work, we assume the linear functional form of $f(Q,T)$ as,

$$f(Q,T) = \chi_1\,Q + \chi_2\,T. \tag{20}$$

which in addition to the metric (18), leads to the three non-vanishing and independent gravitational field equations in $f(Q,T)$ gravity expressed as

$$\rho + \frac{\chi_2}{2}(3\rho - P) + \frac{q^2}{r^4} = -\chi_1\left[\frac{\mathcal{H}_0^3 - \mathcal{H}_0 + 2\mathcal{H}_0' r}{\mathcal{H}_0^3 r^2}\right], \tag{21}$$

$$P + \frac{\chi_2}{2}(3P - \rho) - \frac{q^2}{r^4} = -\frac{\chi_1}{r^2}\left[\frac{\mathcal{F}_0 + 2\mathcal{F}_0' r}{\mathcal{F}_0\mathcal{H}_0^2} - 1\right], \tag{22}$$

$$P + \frac{\chi_2}{2}(3P - \rho) + \frac{q^2}{r^4} = -\frac{\chi_1}{\mathcal{F}_0\mathcal{H}_0^3 r}\big[-\mathcal{H}_0'(\mathcal{F}_0 + \mathcal{F}_0' r) + \mathcal{H}_0(\mathcal{F}_0' + \mathcal{F}_0'' r)\big]. \tag{23}$$

The subsequent aim in the present study is to obtain an exact solution for the present isotropic and charged compact stellar system by solving the field equations. So, we need to solve the isotropy condition for $f(Q,T)$-gravity system, which is obtained by subtracting the Eq. (22) from Eq. (23) as,

$$-\frac{\chi_1}{\mathcal{F}_0\mathcal{H}_0^3 r^2}\Big[r(\mathcal{H}_0\mathcal{F}_0'' r - \mathcal{H}_0\mathcal{F}_0' - \mathcal{F}_0'\mathcal{H}_0' r) - F\big(\mathcal{H}_0 - \mathcal{H}_0^3 + \mathcal{H}_0' r\big)\Big] = \frac{2q^2}{r^4} = 2\,\mathcal{E}_2. \tag{24}$$

The above differential Eq. (24) depends on the three unknowns $\mathcal{F}_0$, $\mathcal{H}_0$ and electric field $\mathcal{E}_2$. For this purpose, we consider a well-known potential corresponding to Korkina–Orlyanskii model [97],

$$\mathcal{H}_0 = \sqrt{\frac{2\mathcal{A}r^2 + 1}{\mathcal{A}r^2 + 1}}. \tag{25}$$

Substitute the above potential in master Eq. (24) and we find,

$$\mathcal{F}_0'' - \frac{1}{r\chi_1\left(\mathcal{A}r^2 + 1\right)\left(2\mathcal{A}r^2 + 1\right)}\Big[\chi_1\Big(2\mathcal{A}^2\mathcal{F}_0' r^4 - 2\mathcal{A}^2\mathcal{F}_0 r^3 + 4\mathcal{A}\mathcal{F}_0' r^2 + \mathcal{F}_0'\Big) - 2\mathcal{E}_2\mathcal{F}_0 r\left(2\mathcal{A}r^2 + 1\right)^2\Big] = 0, \tag{26}$$

As we can clearly see that the above differential equation demands a suitable expression for electric field $\mathcal{E}_2$ which could integrate the Eq. (26) perfectly. We would like to mention that $\mathcal{F}_0 = \sqrt{1 + \mathcal{A}r^2}$ is a particular solution of Eq. (26) when $\mathcal{E}_2 = 0$. In this regard, we have assumed $\mathcal{F}_0 = \sqrt{\mathcal{A}\beta r^2 + 1}$ is particular solution of the Eq.(26), where β is constant parameter. By assuming this particular solution, we choose a non-zero expression for electric field $\mathcal{E}_2$ by introducing a charge parameter β as,

$$\mathcal{E}_2 = \frac{\mathcal{A}^2(\beta - 1)r^2\chi_1\left(4\mathcal{A}\beta r^2 + \beta + 2\right)}{2\left(2\mathcal{A}r^2 + 1\right)^2\left(\mathcal{A}\beta r^2 + 1\right)^2}. \tag{27}$$

It is clearly noted that when $\beta = 1$, then the electric field will disappear while it is positive when $\beta < 1$ as χ_1 is negative. After plugging the electric field expression (27), we use the

change of dependent variable method and find final form of differential equation,

$$\mathcal{F}_0'' - \frac{1}{\left(2\mathcal{A}^2r^5+3\mathcal{A}r^3+r\right)\left(\mathcal{A}\beta r^2+1\right)^2}\Big[\left(\mathcal{A}\beta r^2+1\right)^2 \times\left(2\mathcal{A}^2r^4+4\mathcal{A}r^2+1\right)\mathcal{F}_0' - \beta\,\mathcal{A}^2r^3\left(2\mathcal{A}^2\beta r^4 +4\mathcal{A}\beta r^2+\beta+1\right)\mathcal{F}_0\Big]=0. \tag{28}$$

After solution the above Eq. (28), we get an exact close form solution as,

$$\mathcal{F}_0 = \frac{\sqrt{\mathcal{A}\beta r^2+1}}{(\beta-1)\beta}\Big[(\beta-1)\Big(\beta\,\mathcal{C}_1 - \sqrt{2}\,\mathcal{C}_2\log\big[\sqrt{2\mathcal{A}r^2+1} -\sqrt{2\mathcal{A}r^2+2}\big]\Big) + \mathcal{C}_2\sqrt{\beta^2-3\beta+2} \times\tanh^{-1}\left(\frac{1}{\sqrt{\beta^2-3\beta+2}}\Big[\sqrt{2}\beta\mathcal{A}r^2 - \beta\sqrt{2\mathcal{A}r^2+1} \times\sqrt{\mathcal{A}r^2+1}+\sqrt{2}\Big]\right)\Big]. \tag{29}$$

Since, we have found a complete solution for $f(Q,T)$-system, then we only need to find the explicit expressions for density ρ, and pressure P. By solving of Eqs. (21) and (22), we get an expression for ρ and P as,

$$\rho = -\frac{1}{\mathcal{F}_0\mathcal{H}_0^3r^2\left(2\chi_2^2+3\chi_2+1\right)}\Big[\chi_1\Big(\chi_2\big[\mathcal{F}_0'\mathcal{H}_0r+\mathcal{F}_0 \times\left(3\mathcal{H}_0'r+\mathcal{H}_0^3-\mathcal{H}_0\right)\big]+\mathcal{F}_0\left(2\mathcal{H}_0'r+\mathcal{H}_0^3-\mathcal{H}_0\right)\Big) +\mathcal{E}_2\mathcal{F}_0\mathcal{H}_0^3r^2\left(\chi_2+1\right)\Big], \tag{30}$$

$$P = \frac{1}{\mathcal{F}_0\mathcal{H}_0^3r^2\left(2\chi_2^2+3\chi_2+1\right)}\Big[\chi_1\Big(\mathcal{H}_0\big[\mathcal{F}_0\left(\mathcal{H}_0^2-1\right) -2\mathcal{F}_0'r\big]-\chi_2\left\{3\mathcal{F}_0'\mathcal{H}_0r+\mathcal{F}_0\left(\mathcal{H}_0'r-\mathcal{H}_0^3+\mathcal{H}_0\right)\right\}\Big) +\mathcal{E}_2\mathcal{F}_0\mathcal{H}_0^3r^2\left(\chi_2+1\right)\Big]. \tag{31}$$

After inserting the expressions for $\mathcal{H}_0$, $\mathcal{E}_2$ and $\mathcal{F}_0$ from Eqs. (25), (27), and (29) into Eqs. (30) and (31), we find final expression for ρ and P as,

$$\rho = -\chi_1\Big[\chi_2\Big(2\mathcal{F}_1(r)\left[2\mathcal{A}^2r^4+3\mathcal{A}r^2+1\right]\left(\mathcal{A}\beta r^2+1\right)^2 +\mathcal{A}\mathcal{F}_0r\left[4\mathcal{A}^2\beta(3\beta+1)r^4+\mathcal{A}\left(\beta^2+17\beta+2\right)r^2 +4\mathcal{A}^3\beta^2r^6+8\right]\Big)+\mathcal{A}\mathcal{F}_0r\Big(4\mathcal{A}^3\beta^2r^6+2\mathcal{A}^2\beta(5\beta+2)r^4 +\mathcal{A}\left(\beta^2+13\beta+2\right)r^2+6\Big)\Big]\Big/\Big[2\mathcal{F}_0r\left(2\chi_2^2+3\chi_2+1\right) \times\left(2\mathcal{A}r^2+1\right)^2\left(\mathcal{A}\beta r^2+1\right)^2\Big], \tag{32}$$

$$P = -\chi_1\Big[\chi_2\Big(6\mathcal{F}_1(r)\left(2\mathcal{A}^2r^4+3\mathcal{A}r^2+1\right)\left(\mathcal{A}\beta r^2+1\right)^2 -\mathcal{A}^2\mathcal{F}_0r^3\left(4\mathcal{A}\beta r^2+\left(2\mathcal{A}\beta r^2+\beta\right)^2+\beta+2\right)\Big)+4\mathcal{F}_1(r) \times\left(2\mathcal{A}^2r^4+3\mathcal{A}r^2+1\right)\left(\mathcal{A}\beta r^2+1\right)^2-\mathcal{A}\mathcal{F}_0r\Big(4\mathcal{A}^3\beta^2r^6 +2\mathcal{A}^2\beta(3\beta+2)r^4+\mathcal{A}\left(\beta^2+5\beta+2\right)r^2+2\Big)\Big]\Big/\Big[2\mathcal{F}_0r \times\left(2\chi_2^2+3\chi_2+1\right)\left(2\mathcal{A}r^2+1\right)^2\left(\mathcal{A}\beta r^2+1\right)^2\Big]. \tag{33}$$

where, $\mathcal{F}_1 = \frac{d\mathcal{F}_0}{dr}$ whose expression is given in appendix.

4 Matching condition for the charged stellar system

The stellar matter configuration at the boundary ($r = R$) of any spherically symmetric and stable astrophysical compact object should be smooth and continuous between the interior solution ($r < R$) and the exterior solution ($r > R$). The space-time geometry is physically attainable due to the matching condition at the surface. For the charged system, the Reissner–Nordstrom de-Sitter exterior space-time is taken into account to represent the exterior space-time of the present stellar system. So, we have the exterior space-time metric as

$$dS_+^2 = -\Big(1-\frac{2\mathcal{M}}{r}+\frac{\mathbb{Q}^2}{r^2}+\frac{\Lambda r^2}{3}\Big)dt^2+r^2(d\theta^2+\sin^2\theta \times d\phi^2)+\Big(1-\frac{2\mathcal{M}}{r}+\frac{\mathbb{Q}^2}{r^2}+\frac{\Lambda r^2}{3}\Big)^{-1}dr^2, \tag{34}$$

which is obtained as a static solution to the Einstein-Maxwell field equations and can be regarded as the representation of the gravitational field exterior to a charged and spherically symmetric gravitating body of mass $\mathcal{M}$ and total charge $\mathbb{Q}$.

However, interior metric of the star can be expressed in the most general form by the following space-time metric given as

$$dS_-^2 = -\mathcal{F}_0^2\,dt^2+\mathcal{H}_0^2\,dr^2+r^2(d\theta^2+\sin^2\theta\,d\phi^2). \tag{35}$$

Now, the inner manifold dS_-^2 (35) should be matched with the outer manifold dS_+^2 (35) smoothly at the surface Σ in case of the stable configuration. The first and second fundamental forms along the boundary Σ can be obtained by process of continuity of both the geometries at this Σ. Hence, the first fundamental form can be expressed as

$$g_{tt}^-|_{r=r_\Sigma} = g_{tt}^+|_{r=r_\Sigma} \quad \& g_{rr}^-|_{r=r_\Sigma} = g_{rr}^+|_{r=r_\Sigma}. \tag{36}$$

and can be expressed in the explicit form using Eqs. (35) and (35) as,

$$\mathcal{F}_0^2(R) = \left(1-\frac{2\mathcal{M}}{R}+\frac{\mathbb{Q}^2}{R^2}+\frac{\Lambda R^2}{3}\right), \tag{37}$$

$$\mathcal{H}_0^{-2}(R) = \left(1-\frac{2\mathcal{M}}{R}+\frac{\mathbb{Q}^2}{R^2}+\frac{\Lambda R^2}{3}\right). \tag{38}$$

Furthermore, the second fundamental form expressed in the form,

$$P(R) = 0. \tag{39}$$

With presence of the effect of the electric field, the electric charge is expected to be continuous along the boundary r_Σ

representing

$$q(r)|_{r=R} = \mathbb{Q}, \tag{40}$$

where $q(r)$ is the amount of electric charge present into the fluid sphere. We would like to mention that the observational value of cosmological constant Λ is $(10^{-46}/km^2)$ which has negligible effect on the properties of compact stars. Therefore, we have ignored the cosmological constant Λ in our discussion of compact stars.

$$\begin{aligned}
\mathcal{C}_2 = (\beta-1)\beta\sqrt{\frac{2\mathcal{A}R^2+1}{\mathcal{A}R^2+1}}\Bigg[\sqrt{\mathcal{A}\beta R^2+1}\\
\times\Bigg((\beta-1)\left(\beta \mathrm{C1C2}-\sqrt{2}\log\left(\sqrt{2\mathcal{A}R^2+1}\right.\right.\\
\left.\left.-\sqrt{2\mathcal{A}R^2+2}\right)\right)+\sqrt{\beta^2-3\beta+2}\\
\times\tanh^{-1}\left(\frac{\sqrt{2}\mathcal{A}\beta R^2-\beta\sqrt{\mathcal{A}R^2+1}\sqrt{2\mathcal{A}R^2+1}+\sqrt{2}}{\sqrt{\beta^2-3\beta+2}}\right)\Bigg)\Bigg]^{-1},\\
\mathcal{C}_1 = \mathcal{C}_3(\beta-1)\beta\sqrt{\frac{2\mathcal{A}R^2+1}{\mathcal{A}R^2+1}}\Bigg[\sqrt{\mathcal{A}\beta R^2+1}\\
\times\Bigg((\beta-1)\left(\beta \mathrm{C1C2}-\sqrt{2}\log\left(\sqrt{2\mathcal{A}R^2+1}\right.\right.\\
\left.\left.-\sqrt{2\mathcal{A}R^2+2}\right)\right)+\sqrt{\beta^2-3\beta+2}\\
\times\tanh^{-1}\left(\frac{\sqrt{2}\mathcal{A}\beta R^2-\beta\sqrt{\mathcal{A}R^2+1}\sqrt{2\mathcal{A}R^2+1}+\sqrt{2}}{\sqrt{\beta^2-3\beta+2}}\right)\Bigg)\Bigg]^{-1}.
\end{aligned}$$

5 Physical features of the present model

5.1 Charge

It is expected that a physical charged stellar system should fulfill the conditions validating the physical acceptance of the stellar model as described in a study [98]. The regularity of the proper charge density at the center of the stellar configuration has been explored to be an essential requirement in connection to the physical behavior of electromagnetic field in a work [99]. This can be considered to be a basic feature with regard to the application of charged stellar model. So, we have examined the physical validity of the electric field by investigating the nature of charge function with respect to coupling constants χ_1, χ_2 and charge parameter β. The behavior of charge has been shown graphically in Fig. 1.

It can be inferred from Fig. 1 that the charge vanishes at the center of the stellar configuration for the changing values of the parameters. Further, the increasing nature of the charge is prominent throughout the configuration for all the cases. The charge reaches its maximum value at the surface of the star. The surface charge does not depend on the parameter χ_2. However, it increases with increasing values of χ_1 and decreases with increasing values of β. Evidently, the non-metricity scalar and charge parameters have a significant effect on the intensity of the electric field in the present stellar system.

It can be seen that the amount of charge remains at a minimum and almost constant value near the central region of the star and then starts to increase rapidly after some critical distance from the center. Physically, this fact implies that the charged particles have a high tendency to wander and reside away from the central region of the stellar configuration. The values of surface charge for different values of parameters have been provided in Tables 1, 2 and 3. We find that the surface charge lies in the range $[4.4\times10^{19}, 9.9\times10^{19}]$ coulomb for all the parameters. Research studies [100–102] explored similar features of the charge function for the isotropic stellar systems in embedding class one spacetime in the framework of GR with the surface charge of the order of 10^{20} C.

Now, we make an effort to justify the presence of the amount of charge based on the available research studies. For instance, a study [99] indicated that the net charge at the fluid-vacuum interface, i.e., the boundary can be of the order of 10^{19} C for the stars having dissipation of charge along the surface of the star. Moreover, in order to attain force equilibrium with the physical consequences of charge a stellar configuration like a neutron star can hold a large amount of charge of the order of 10^{20} C as shown by numerical calculations in [81]. The presence of repulsive electric force due to positively charged particles in the self-gravitating compact objects is one of the physical implications of charge which offers resistance to the gravitational collapse of the self-gravitating bodies [86,103].

5.2 Density and pressure

The energy density as well as the isotropic pressure of the stellar system in the present gravitational model have been verified graphically in the Figs. 2 and 3. Both the density and isotropic pressure have finite central values for the changing values of the parameters χ_1, χ_2, and β. This confirms that the obtained exact solution is non-singular having regular behavior at the center. Density and pressure possess a decreasing nature with respect to radial distance. Notably, variations in the effects of the parameters on the physical behavior of density and pressure can be seen in characteristic ways.

The charge parameter has no effect on the density but influences the pressure substantially. Again, an increase in χ_1 leads to higher density and pressure as the similar effect of χ_1 on the charge. However, parameter χ_2 effects the density and pressure in a distinct way. Enhanced values of χ_2 have a reducing influence on the density but a rising impact on the pressure. It is important to note that the vanishing condition of isotropic pressure is satisfied for all cases. The values of central pressure which are shown in Tables 1, 2 and 3 have

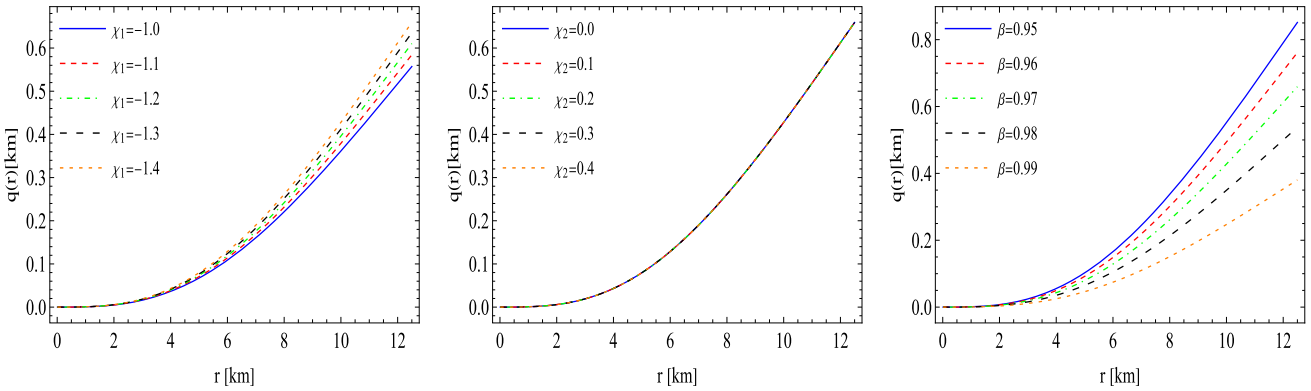

Fig. 1 Impact of $f(Q,T)$ parameters χ_1 and χ_2, and charge parameter β on the electric charge configuration $(q(r))$ versus radial distance r for $\mathcal{A} = 0.003\text{km}^{-2}$ with fixed values: (i) $\chi_1 = -1.4$ and $\beta = 0.97$ for left panel, (ii) $\chi_2 = 0.3$ and $\beta = 0.97$ for middle panel, and (iii) $\chi_1 = -1.4$ and $\chi_2 = 0.3$ for right panel

Table 1 The study of physical values for different $f(Q,T)$ parameter χ_1 with fixed values of $A = 0.003\ \text{km}^{-2}$, $\chi_2 = 0.3$, and $\beta = 0.97$

χ_1	Central pressure $(P_r)_c^{\text{eff}}\ (dyne/cm^2)$	Central density $\rho_c^{\text{eff}}\ (gm/cm^3)$	Surface density $\rho_s^{\text{eff}}\ (gm/cm^3)$	Adiabatic index Γ_c	Charge (in Coulomb) $\mathbb{Q}(C)$
−1.0	3.36733×10^{34}	3.3718×10^{14}	1.16066×10^{14}	1.66223	6.49618×10^{19}C
−1.1	3.70407×10^{34}	3.70898×10^{14}	1.27673×10^{14}	1.66223	6.81325×10^{19}C
−1.2	4.0408×10^{34}	4.04616×10^{14}	1.3928×10^{14}	1.66223	7.11621×10^{19}C
−1.3	4.37753×10^{34}	4.38334×10^{14}	1.50886×10^{14}	1.66223	7.40678×10^{19}C
−1.4	4.71427×10^{34}	4.72052×10^{14}	1.62493×10^{14}	1.66223	7.68638×10^{19}C

Table 2 The study of physical values for different $f(Q,T)$ parameter χ_2 with fixed values of $A = 0.003\ \text{km}^{-2}$, $\chi_1 = -1.4$, and $\beta = 0.97$

χ_2	Central pressure $(P_r)_c^{\text{eff}}\ (dyne/cm^2)$	Central density $\rho_c^{\text{eff}}\ (gm/cm^3)$	Surface density $\rho_s^{\text{eff}}\ (gm/cm^3)$	Adiabatic index Γ_c	Charge (in Coulomb) $\mathbb{Q}(C)$
0.0	3.511×10^{34}	6.7662×10^{14}	2.35615×10^{14}	1.45540	7.68638×10^{19}C
0.1	4.23827×10^{34}	5.90412×10^{14}	2.04882×10^{14}	1.56579	7.68638×10^{19}C
0.2	4.58007×10^{34}	5.24391×10^{14}	1.81242×10^{14}	1.62453	7.68638×10^{19}C
0.3	4.71427×10^{34}	4.72052×10^{14}	1.62493×10^{14}	1.66223	7.68638×10^{19}C
0.4	4.73205×10^{34}	4.29458×10^{14}	1.47259×10^{14}	1.68888	7.68638×10^{19}C

Table 3 The effect of charge parameter β on physical parameters with fixed values of $A = 0.003\ \text{km}^{-2}$, $\chi_1 = -1.4$, and $\chi_2 = 0.3$

β	Central pressure $(P_r)_c^{\text{eff}}\ (dyne/cm^2)$	Central density $\rho_c^{\text{eff}}\ (gm/cm^3)$	Surface density $\rho_s^{\text{eff}}\ (gm/cm^3)$	Adiabatic index Γ_c	Charge (in Coulomb) $\mathbb{Q}(C)$
0.95	4.45699×10^{34}	4.71756×10^{14}	1.62052×10^{14}	1.63752	9.9273×10^{19}C
0.96	4.58541×10^{34}	4.71904×10^{14}	1.62273×10^{14}	1.64989	8.87739×10^{19}C
0.97	4.71427×10^{34}	4.72052×10^{14}	1.62713×10^{14}	1.66223	7.68638×10^{19}C
0.98	4.84354×10^{34}	4.7220×10^{14}	1.62933×10^{14}	1.67454	6.2745×10^{19}C
0.99	4.97323×10^{34}	4.72349×10^{14}	1.47259×10^{14}	1.68684	4.43571×10^{19}C

rising nature for increasing values of the three parameters. Additionally, the numerical values of surface density and central density are given in Tables 1, 2 and 3.

It can be seen from the tables that the density is of the order of 10^{14} g/cm^3 and the pressure is of the order of 10^{34} dyne/cm^2. The values of central density lie in the range $[3.3 \times 10^{14}, 6.7 \times 10^{14}]$ g/cm^3 which suggests that the star is mainly composed of degenerate neutrons in addition with electrons and possibly negative muons [104]. Various research works [100–102] explored similar features of the density and pressure for isotropic stellar systems in embedding class one spacetime in the framework of GR with central density and central pressure of the order of 10^{15} g/cm^3 and 10^{35} dyne/cm^2 respectively. It is also suggested in [104] that the stellar matter may be heterogeneous and hence anisotropic with the presence of hyperons in particular at very high-density regime the of the order 10^{15} g/cm^3. However, the present study predicts densities of the order of 10^{14} g/cm^3 throughout the star which basically supports the isotropic nature of the stellar system.

6 Causality and equation of state

Initially we should investigate the causality condition in the interior of stellar structure. In this regard the sound speed can be expressed as

$$v_r^2 = \frac{dp}{d\rho}. \tag{41}$$

In the perfect fluid configuration, the sound should traverse with a speed less than the speed of light in the interior of star [107] implying the causality condition as $v_r^2 < 1$ where the light speed is unity in the system of the natural unit. The variation in the square of the sound speed for increasing radial distance and changing values of parameters is shown in Fig. 6. Apparently, the sound speed is less than one throughout the stellar configuration for all cases. The causality condition is satisfied in the present gravitational system in the context of $f(Q, T)$ gravity.

It is to be noted that the characteristics of the square of sound speed within the stellar system varies in distinct ways for three cases in Fig. 6. For fixed χ_2 and β the left panel shows that the sound speed increases with non-zero central values and then reaching a maximum value starts to decrease near the surface region. A similar profile of square of sound speed is obtained in a recent work [105] where an isotropic and charged stellar system is studied by assuming Tolman IV type potential. In contrast, the middle panel signifies that the speed of sound remains almost constant with a minimal slope for fixed χ_1 and β. The right panel shows the nature of sound speed similar to the left panel but with comparatively lower values of the gradient. The sound speed is not influenced by the parameter χ_1. On the other hand, an increase in χ_2 and β parameter enhance the sound speed in the stellar system.

The sound speed in the stellar configurations can be analyzed as a good indicator of the stiffness of an equation of state (EOS) of the constituent matter. For instance, it had been claimed by Canuto [106] that the stellar configurations with decreasing sound speed near the surface region have an ultra-high distribution of matter. Again, increasing sound speed implies stiffer EOS. On the other hand, EOS softens in the regions inside the star where the sound travels with minimum speed. Based on this discussion, it can be argued that the fixed values of χ_2 and β parameters can impact the stiffness of EOS in distinct ways inside the star.

7 Adiabatic condition of stability

It is important to perform a physical test to examine the stable equilibrium of the present stellar model under the influence of parameters χ_1, χ_2, and β. In this connection, the adiabatic index for a perfect fluid is expressed as

$$\Gamma = \left(\frac{\rho + p}{p}\right)\left[\frac{dp}{d\rho}\right]. \tag{42}$$

A stable stellar configuration has an adiabatic index greater than 4/3. This is a stability condition in terms of the adiabatic index as discussed in the studies [108–110]. We have investigated the adiabatic index and shown the graphical presentation of Γ for changing values of parameters in Fig. 5. The central values as displayed both in Fig. 5 and Tables 1, 2 and 3 are greater than 4/3 for changing values parameters. Moreover, the adiabatic index has an increasing nature with respect to radial distance and reaches a maximum value at the surface for all cases. Hence the adiabatic condition of stability is fulfilled in the present gravitational configuration in $f(Q, T)$ gravity. There is no effect of χ_1 on the adiabatic index. However, the adiabatic index increases with increasing values of χ_2 and β which indicates that the presence of charge and coupling of a trace of energy–momentum tensor enables the gravitational systems to be in stable equilibrium.

8 Mass-radius relationship in $f(Q, T)$ gravity

The $f(Q, T)$ gravitational theory could be considered as a more physical framework for modeling realistic compact stars, regardless of the success of other modified theories in the field of astrophysics and cosmology. It includes a non-metricity tensor, a geometric property combined with the trace of energy–momentum of matter, which offers interactions describing the physical features of highly dense gravitating objects like compact stars. Additionally, the modified field equations with non-metricity effects can describe the

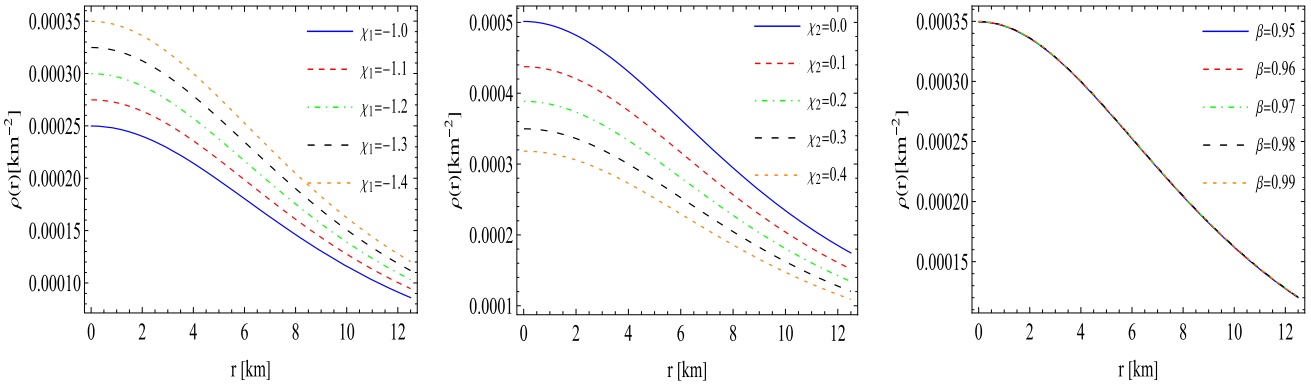

Fig. 2 Impact of $f(Q,T)$ parameters χ_1 and χ_2, and charge parameter β on the energy density ($\rho(r)$) versus radial distance r for $\mathcal{A} = 0.003\text{km}^{-2}$ with fixed values: (i) $\chi_1 = -1.4$ and $\beta = 0.97$ for left panel, (ii) $\chi_2 = 0.3$ and $\beta = 0.97$ for middle panel, and (iii) $\chi_1 = -1.4$ and $\chi_2 = 0.3$ for right panel

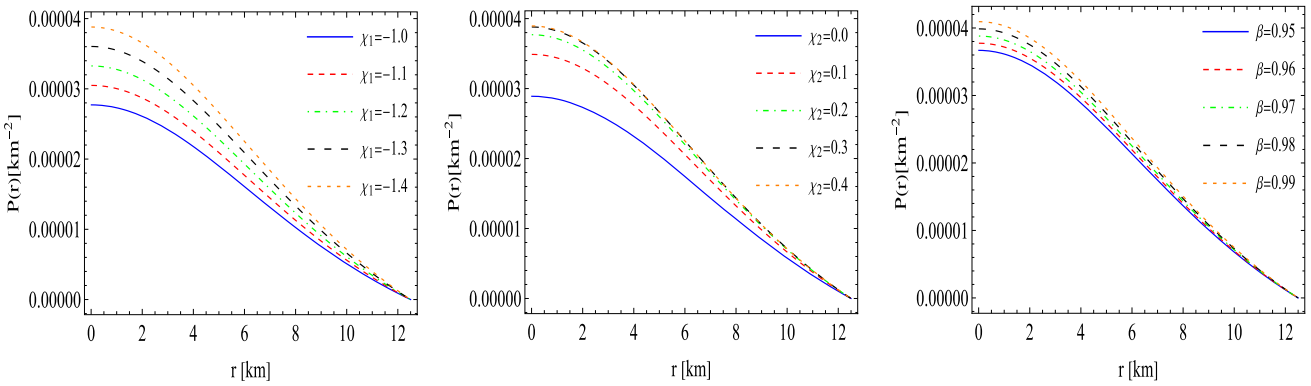

Fig. 3 Impact of $f(Q,T)$ parameters χ_1 and χ_2, and charge parameter β on the pressure ($P(r)$) versus radial distance r for $\mathcal{A} = 0.003\text{km}^{-2}$ with same fixed values mentioned in Fig. 2

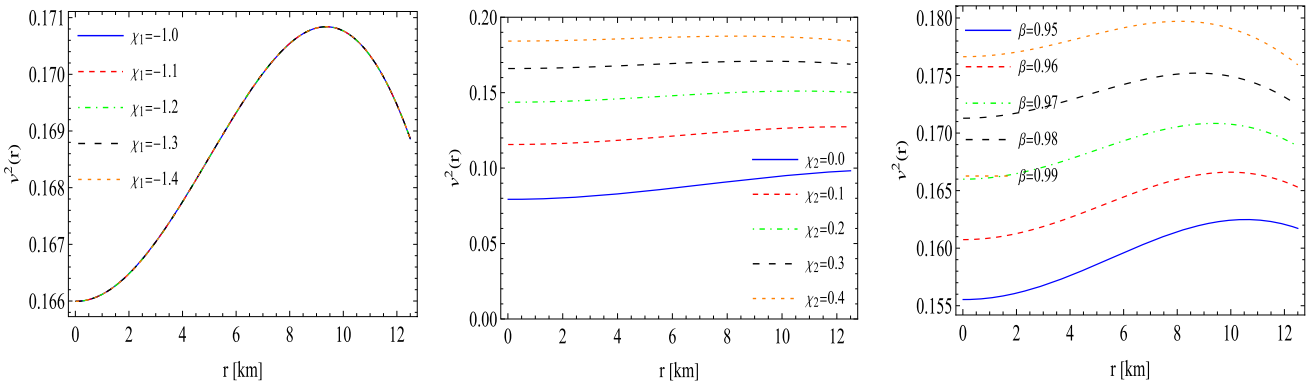

Fig. 4 Impact of $f(Q,T)$ parameters χ_1 and χ_2, and charge parameter β on the velocity of sound ($v^2(r)$) versus radial distance r for $\mathcal{A} = 0.003\text{km}^{-2}$ with same fixed values mentioned in Fig. 2

stellar structure comprehensively leading to various predictions for mass-radius relation and stability of compact stars. By examining the mass-radius relation compatible with the observational constraints of the stars we can inspect the applicability of $f(Q,T)$ gravity with its theoretical aspects on the modeling of compact stars.

We examine the mass-radius relation of the isotropic charged stellar system with the influence of coupling constants χ_1, χ_2, and charge parameter β in the context of $f(Q,T)$ gravity. With this regard, we have shown the $M-R$ curves for various values of χ_1, χ_2, and β in the three panels of Fig. 6. The $M-R$ curves in each panel of Fig. 6 have increasing nature with respect to radius and after reaching

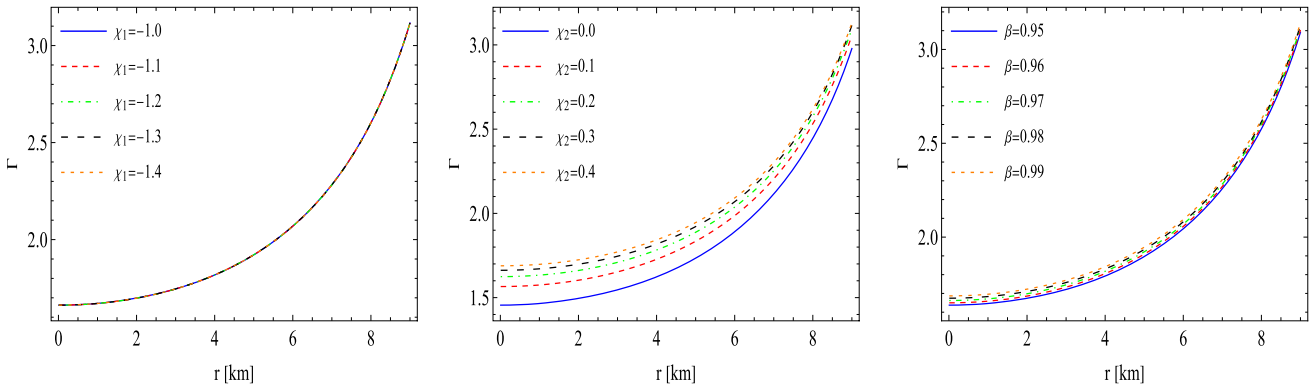

Fig. 5 Impact of $f(Q,T)$ parameters χ_1 and χ_2, and charge parameter β on the adiabatic index $[\Gamma(r)]$ versus radial distance r for $\mathcal{A} = 0.003\text{km}^{-2}$ with same fixed values mentioned in Fig. 2

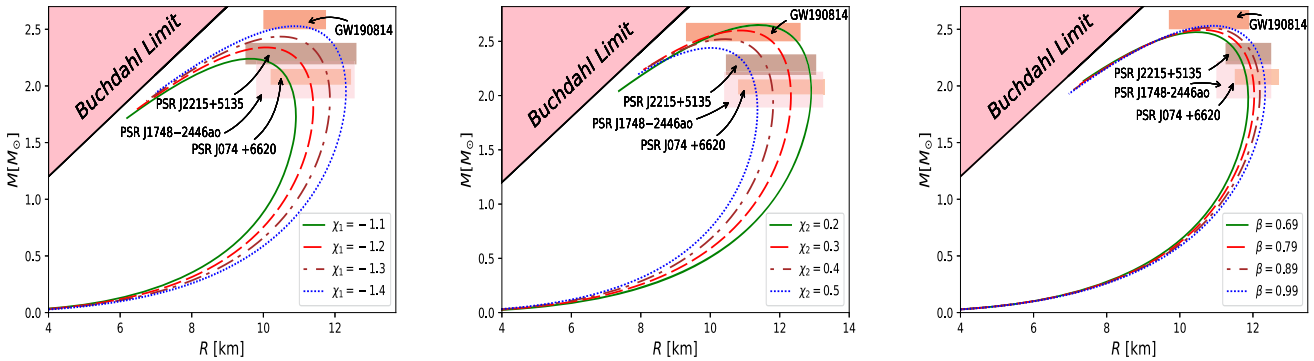

Fig. 6 Impact of $f(Q,T)$ parameters χ_1 and χ_2, and charge parameter β on the total mass-radius relation for $\mathcal{A} = 0.003\text{km}^{-2}$ with same fixed values mentioned in Fig. 2

Table 4 Numerical values of the predicted radii of massive observed stars with respect to χ_1 corresponding to left panel of Fig. 6

Objects	$\frac{M}{M_\odot}$	Predicted R (km)			
		χ_1			
		−1.1	−1.2	−1.3	−1.4
PSR J074 +6620 [113]	2.08 ± 0.07	$10.63^{-0.22}_{+0.12}$	$11.26^{-0.11}_{+0.06}$	$11.79^{-0.06}_{+0.04}$	$12.28^{-0.03}_{+0.02}$
PSR J2215+5135 [114]	$2.28^{+0.10}_{-0.09}$	10.27	$10.78_{+0.29}$	$11.52^{-0.34}_{+0.16}$	$12.12^{-0.19}_{+0.10}$
PSR J1748-2446ao [115]	$2.16^{+0.06}_{-0.27}$	$10.42^{+0.44}_{+0.27}$	$11.14^{-0.14}_{+0.24}$	$11.72^{-0.08}_{+0.14}$	$12.24^{-0.06}_{+0.06}$
GW190814 [116]	2.5–2.67	–	–	–	11.39

Table 5 Numerical values of the predicted radii of massive observed stars with respect to χ_2 corresponding to middle panel of Fig. 6

Objects	$\frac{M}{M_\odot}$	Predicted R (km)			
		χ_2			
		0.2	0.3	0.4	0.5
PSR J074 +6620 [113]	2.08 ± 0.07	$12.90^{-0.01}_{+0.00}$	$12.31^{-0.02}_{+0.0}$	$11.78^{-0.04}_{+0.02}$	$11.29^{-0.06}_{+0.04}$
PSR J2215+5135 [114]	$2.28^{+0.10}_{-0.09}$	$12.82^{-0.10}_{+0.05}$	$12.20^{-0.14}_{+0.07}$	$11.61^{-0.19}_{+0.09}$	$11.03^{-0.32}_{+0.16}$
PSR J1748-2446ao [115]	$2.16^{+0.06}_{-0.27}$	$12.89^{-0.03}_{-0.01}$	$12.28^{-0.03}_{+0.03}$	$11.73^{-0.05}_{+0.08}$	$11.22^{-0.08}_{+0.14}$
GW190814 [116]	2.5-2.67	$12.21_{+0.28}$	$11.32_{+0.45}$	10.87	–

Table 6 Numerical values of the predicted radii of massive observed stars with respect to β corresponding to right panel of Fig. 6

Objects	$\frac{M}{M_\odot}$	Predicted R (km)			
		β			
		0.69	0.79	0.89	0.99
PSR J074 +6620 [113]	2.08 ± 0.07	$11.82^{-0.06}_{+0.03}$	$11.99^{-0.04}_{+0.03}$	$12.16^{-0.04}_{+0.02}$	$12.31^{-0.03}_{+0.02}$
PSR J2215+5135 [114]	$2.28^{+0.10}_{-0.09}$	$11.59^{-0.27}_{+0.13}$	$11.79^{-0.22}_{+0.12}$	$11.98^{-0.21}_{+0.10}$	$12.15^{-0.19}_{+0.10}$
PSR J1748-2446ao [115]	$2.16^{+0.06}_{-0.27}$	$11.75^{-0.06}_{+0.12}$	$11.93^{-0.06}_{+0.10}$	$12.11^{-0.06}_{+0.08}$	$12.27^{-0.05}_{+0.06}$
GW190814 [116]	2.5-2.67	–	–	11.13	11.45

Table 7 Predicted maximum allowable mass and the corresponding radius with respect to the physical model parameters

χ_1	M_{max} $(M_\odot)$	R (km)	χ_2	M_{max} $(M_\odot)$	R (km)	β	M_{max} $(M_\odot)$	R (km)
−1.1	2.24	9.66	0.2	2.65	11.42	0.69	2.47	10.47
−1.2	2.34	10.09	0.3	2.60	10.89	0.79	2.49	10.64
−1.3	2.43	10.49	0.4	2.52	10.44	0.89	2.51	10.78
−1.4	2.53	11.87	0.5	2.44	10.03	0.99	2.53	10.93

the maximum point its starts to decrease. The peak of the $M - R$ curves corresponds to the maximum allowable mass of the compact star in the framework of $f(Q, T)$ gravity. The maximum mass increases with increasing values of χ_1 and β as shown in Fig. 6. However, increasing values of χ_2 have a tendency to decrease maximum mass. This can be justified by the nature of the influence of coupling constants on the density of the stellar system as shown in Fig. 2. So, the combined effect of χ_1 and χ_2 helps the stellar configuration to attain sustainable maximum mass ensuring stable equilibrium. The analysis of the mass-radius relation indicates that the present stellar model fulfills the Buchdahl limit for all the changing values of parameters. This is in concurrence with the physical validation of the present gravitational model.

Measurements of mass of compact stars appear to be straightforward in comparison with techniques of radii determination based on observational constraints [111,112]. To determine the radii of the known observed stars we have considered observed pulsars like PSR J0740+6620 [113], PSR J2215+5135 [114], PSR J1748-2446ao [115] and a secondary companion in GW190814 [116] as candidates of compact stars with known mass. It is worth mentioning that a recent study [115] has measured the mass of PSR J1748-2446ao to be $2.16^{+0.06}_{-0.27}$ $M_\odot$ with 68.3% confidence limit. Further, PSR J1748-2446ao is a possible candidate double neutron star with the longest orbital period. We have shown the predicted radii for the observed stars of masses greater than 2.01 $M_\odot$ in Tables 4, 5 and 6. It has been depicted that the predicted radii are in the range [10.27, 12.90] km. Apparently this predicted radii is highly consistent with the obtained physical radius for various neutron star EOS by Lattimer and Prakash [117].

The predicted radii of the observed stars are seen to be increasing with increased values of χ_1 and β whereas it decreases with increasing values of χ_2. The values of maximum mass and radius corresponding to each peak of $M - R$ curves for various values of parameters have been provided in Table 7. The maximum mass falls in the range [2.24, 2.65] $M_\odot$ with corresponding radii in the range [9.66, 11.87] km as can be seen from Table 7. Since the present model describes the physical star with isotropy in pressure and density of the order of 10^{14} g/cm^3, it can not account for the radii of the star falling in mass gap region for changing values of χ_1 and β with fixed χ_2. Only by decreasing χ_2, a parameter representing the matter part in the non-minimal coupling, can enhance maximum mass in order to predict radii for the stars in mass gap regions like GW190814. In this connection, the radius of the secondary companion in GW190814 is predicted to fall in the range [10.87, 12.49] km by the present isotropic charged stellar model in $f(Q, T)$ gravity.

9 Conclusion

We have obtained a novel exact solution to the modified field equations in context of $f(Q, T)$ gravity for a charged stellar system with isotropic fluid assuming a metric potential ansatz and a well-behaved functional form of the electric field. We have explored various characteristics of the obtained solution by presenting the variation in charge, density and pressure in graphically.

The regularity of the charge function at the center of the stellar configuration has been obtained as an essential requirement in the present model in agreement with the stud-

ies [98,99]. We have examined the physical validity of the electric field by investigating the nature of the charge function with respect to coupling constants χ_1, χ_2, and charge parameter β as shown graphically in Fig. 1. The increasing nature of the charge is prominent throughout the configuration for all the cases. Physically, this fact implies that the charged particles have a high tendency to wander and reside away from the central region of the stellar configuration. The surface charge does not depend on the parameter χ_2. However, it increases with increasing values of χ_1 and decreases with increasing values of β. Evidently, the non-metricity scalar and charge parameters have a significant effect on the intensity of the electric field in the present stellar system. The values of surface charge for different values of parameters have been provided in Tables 1, 2 and 3. We find that the surface charge lie in the range $[4.4 \times 10^{19}, 9.9 \times 10^{19}]$ coulomb for all the parameters. A study [99] indicated that the net charge at the fluid-vacuum interface, i.e., the boundary can be of the order of 10^{19} C for the stars having dissipation of charge along the surface of the star. The presence of repulsive electric force due to positively charged particles in the self-gravitating compact objects is one of the physical implications of charge which offers resistance to the gravitational collapse of the self-gravitating bodies [86,103].

The energy density as well as the isotropic pressure of the stellar system in the present gravitational model have been verified graphically in the Figs. 2 and 3. Both the density and isotropic pressure have finite central values for the changing values of the parameters χ_1, χ_2, and β. This confirms that the obtained exact solution is non-singular having regular behavior at the center. Density and pressure possess a decreasing nature with respect to radial distance. The charge parameter has no effect on the density but influences the pressure substantially. Again, an increase in χ_1 leads to higher density and pressure as a similar effect of χ_1 on the charge. However, parameter χ_2 affects the density and pressure in a distinct way. Enhanced values of χ_2 have a reducing influence on the density but a rising impact on the pressure. It is important to note that the vanishing condition of isotropic pressure is satisfied for all cases. The values of central pressure which are shown in Tables 1, 2 and 3 have rising nature for increasing values of the three parameters. Additionally, the numerical values of surface density and central density are given in Tables 1, 2 and 3.

It can be seen from the tables that the density is of the order of 10^{14} g/cm^3 and the pressure is of the order of 10^{34} dyne/cm^2. The values of central density lie in the range $[3.3 \times 10^{14}, 6.7 \times 10^{14}]$ g/cm^3 which suggests that the star is mainly composed of degenerate neutrons in addition with electrons and possibly negative muons [104]. Various research works [100–102] explored similar features of the density and pressure for isotropic stellar systems in embedding class one spacetime in the framework of GR with central density and central pressure of the order of 10^{15} g/cm^3 and 10^{35} dyne/cm^2 respectively. It is also suggested in [104] that the stellar matter may be heterogeneous and hence anisotropic with the presence of hyperons in particular at a very high-density regime of the order 10^{15} g/cm^3. However, the present study predicts densities of the order of 10^{14} g/cm^3 throughout the star which basically supports the isotropic nature of the stellar system.

The variation in the square of the sound speed for increasing radial distance and changing values of parameters is shown in Fig. 4. Apparently, the sound speed is less than one throughout the stellar configuration for all cases. The causality condition is satisfied in the present gravitational system in the context of $f(Q, T)$ gravity.

The characteristics of the square of sound speed within the stellar system vary in distinct ways for three cases in Fig. 4. For fixed χ_2 and β the left panel shows that the sound speed increases with non-zero central values and then reaching a maximum value starts to decrease near the surface region. A similar profile of square of sound speed is obtained in a recent work [105] where an isotropic and charged stellar system is studied by assuming Tolman IV type potential. In contrast, the middle panel signifies that the speed of sound remains almost constant with a minimal slope for fixed χ_1 and β. The right panel shows the nature of sound speed similar to the left panel but with comparatively lower values of the gradient. The sound speed is not influenced by the parameter χ_1. On the other hand, an increase in χ_2 and β parameter enhance the sound speed in the stellar system. It can be argued [106] that the fixed values of χ_2 and β parameters can impact the stiffness of EOS in distinct ways inside the star.

We have studied the adiabatic condition of stability [108–110] and shown the adiabatic index the graphical presentation of Γ for changing values of parameters in the Fig. 5. The central values as displayed both in Fig. 5 and Tables 1, 2 and 3 are greater than 4/3 for changing values parameters. Moreover, the adiabatic index has an increasing nature with respect to radial distance and reaches a maximum value at the surface for all cases. Hence the adiabatic condition of stability is satisfied in the present gravitational configuration in $f(Q, T)$ gravity. There is no effect of χ_1 on the adiabatic index. However, the adiabatic index increases with increasing values of χ_2 and β which indicates that the presence of charge and coupling of the trace of energy–momentum tensor enables the gravitational systems to be in stable equilibrium.

We have examined the mass-radius relation of the isotropic charged stellar system with the effect of coupling constants χ_1, χ_2, and charge parameter β in the context of $f(Q, T)$ gravity. With this regard, we have shown the $M - R$ curves for various values of χ_1, χ_2, and β in the three panels of Fig. 6. The analysis of the mass-radius relation indicates that the present stellar model fulfills the Buchdahl limit for all the changing values of parameters. The $M - R$ curves in each

panel of Fig. 6 have increasing nature with respect to radius and after reaching the maximum point it starts to decrease. The peak of the $M-R$ curves corresponds to the maximum allowable mass of the compact star in the framework of $f(Q,T)$ gravity. The maximum mass increases with increasing values of χ_1 and β as shown in Fig. 6. However, increasing values of χ_2 have a tendency to decrease maximum mass. This can be justified by the nature of the influence of coupling constants on the density of the stellar system as shown in Fig. 2. So, the combined effect of χ_1 and χ_2 helps the stellar configuration to attain sustainable maximum mass ensuring stable equilibrium.

We have predicted the radii of the known observed stars such as observed pulsars like PSR J0740+6620 [113], PSR J2215+5135 [114], PSR J1748-2446ao [115] and a secondary companion in GW190814 [116] of masses greater than 2.01 $M_\odot$ and shown the predicted radii for the observed stars in Tables 4, 5 and 6. It has been depicted that the predicted radii are in the range [10.27, 12.90] km which is highly consistent with the obtained physical radius for various neutron star EOS [117].

The predicted radii of the observed stars are seen to be increasing with increased values of χ_1 and β whereas it decreases with increasing values of χ_2. The values of maximum mass and radius corresponding to each peak of $M-R$ curves for various values of parameters have been provided in Table 7. The maximum mass falls in the range [2.24, 2.65] $M_\odot$ with corresponding radii in the range [9.66, 11.87] km as can be seen from Table 7. Since the present model describes the physical star with isotropy in pressure and density of the order of 10^{14} g/cm^3, it can not account for the radii of the star falling in mass gap region for changing values of χ_1 and β with fixed χ_2. Only by decreasing χ_2, a parameter representing the matter part in the non-minimal coupling, can enhance maximum mass in order to predict radii for the stars in mass gap regions like GW190814. In this connection, the radius of the secondary companion in GW190814 is predicted to fall in the range [10.87, 12.49] km by the present isotropic charged stellar model in $f(Q,T)$ gravity.

As a final comment, it is to be noted that an isotropic charged stellar configuration has been explored successfully in the context of $f(Q,T)$ gravity with a detailed analysis of the influence of non-minimal coupling between the geometric part Q and matter part T.

Acknowledgements The authors F. Al Khayari and S. K. Maurya acknowledge that this research work is supported by the TRC Project (Grant No. BFP/GRG/CBS/23/072). The authors are also thankful for the continuous support and encouragement from the administration of the University of Nizwa for this research work.

Data Availability Statement This manuscript has no associated data. [Authors' comment: Data sharing is not applicable to this article as no datasets were generated or analyzed during the current study. The current work has already included a comprehensive analysis and the corresponding calculations.]

Code Availability Statement This manuscript has no associated code/software. [Authors' comment: This is a theoretical work, and no new code/software has been generated. The numerical computation has been performed using Mathematica and Python software.]

Funded by SCOAP^3.

Appendix

$$
\begin{aligned}
\mathcal{C}_3 = -\Bigg[&(\beta-1)\Big(\left(4\mathcal{A}^3\beta^2R^6+2\mathcal{A}^2\beta(3\beta+2)R^4\right.\\
&\left.+\mathcal{A}\left(3\beta^2+7\beta-2\right)R^2+4\beta-2\right)\\
&\times\log\left(\sqrt{2\mathcal{A}R^2+1}-\sqrt{2\mathcal{A}R^2+2}\right)\\
&\times\left(-16\mathcal{A}^2R^4+2\mathcal{A}\left(4\sqrt{2\mathcal{A}R^2+1}\sqrt{2\mathcal{A}R^2+2}-13\right)R^2\right.\\
&\left.+7\sqrt{2\mathcal{A}R^2+1}\sqrt{2\mathcal{A}R^2+2}-10\right)\\
&+4\left(2\mathcal{A}^2R^4+3\mathcal{A}R^2+1\right)\\
&\times\beta\left(\mathcal{A}\beta R^2+1\right)\left(-16\mathcal{A}^2R^4\right.\\
&+2\mathcal{A}\left(4\sqrt{2\mathcal{A}R^2+1}\sqrt{2\mathcal{A}R^2+2}\right.\\
&\left.\left.-11\right)R^2+5\sqrt{2\mathcal{A}R^2+1}\sqrt{2\mathcal{A}R^2+2}-7\right)\Big)\\
&+\left(4\mathcal{A}^3\beta^2R^6+2\mathcal{A}^2\beta(3\beta+2)R^4\right.\\
&\left.+\mathcal{A}\left(3\beta^2+7\beta-2\right)R^2+4\beta-2\right)\\
&\times\tanh^{-1}\left(\frac{\mathcal{A}\beta\sqrt{2}R^2-\sqrt{\mathcal{A}R^2+1}\sqrt{2\mathcal{A}R^2+1}\beta+\sqrt{2}}{\sqrt{\beta^2-3\beta+2}}\right)\\
&\times\left(8\mathcal{A}^2\sqrt{2}R^4+\mathcal{A}\left(13\sqrt{2}-8\sqrt{\mathcal{A}R^2+1}\sqrt{2\mathcal{A}R^2+1}\right)R^2\right.\\
&\left.+5\sqrt{2}-7\sqrt{\mathcal{A}R^2+1}\sqrt{2\mathcal{A}R^2+1}\right)\sqrt{\beta^2-3\beta+2}\\
&+\Bigg[(\beta-1)\Big(\left(8\mathcal{A}^3\beta^2R^6+2\mathcal{A}^2\beta(7\beta+4)R^4\right.\\
&\left.+\mathcal{A}\left(5\beta^2+17\beta-2\right)R^2+6\beta\right)\log\left(\sqrt{2\mathcal{A}R^2+1}\right.\\
&\left.-\sqrt{2\mathcal{A}R^2+2}\right)\\
&\times\left(-16\mathcal{A}^2R^4+2\mathcal{A}\left(4\sqrt{2\mathcal{A}R^2+1}\sqrt{2\mathcal{A}R^2+2}-13\right)R^2\right.\\
&\left.+7\sqrt{2\mathcal{A}R^2+1}\sqrt{2\mathcal{A}R^2+2}-10\right)
\end{aligned}
$$

$$
\begin{aligned}
&+6\left(2\mathcal{A}^2R^4+3\mathcal{A}R^2+1\right)\\
&\times\beta\left(\mathcal{A}\beta R^2+1\right)\left(-16\mathcal{A}^2R^4\right.\\
&+2\mathcal{A}\left(4\sqrt{2\mathcal{A}R^2+1}\sqrt{2\mathcal{A}R^2+2}-11\right)R^2\\
&\left.+5\sqrt{2\mathcal{A}R^2+1}\sqrt{2\mathcal{A}R^2+2}-7\right)\Big)\\
&+\left(8\mathcal{A}^3\beta^2R^6+2\mathcal{A}^2\beta(7\beta+4)R^4+\mathcal{A}\left(5\beta^2+17\beta-2\right)R^2\right.\\
&\left.+6\beta\right)\tanh^{-1}\left(\frac{\mathcal{A}\beta\sqrt{2}R^2-\sqrt{\mathcal{A}R^2+1}\sqrt{2\mathcal{A}R^2+1}\beta+\sqrt{2}}{\sqrt{\beta^2-3\beta+2}}\right)\\
&\times\left(8\mathcal{A}^2\sqrt{2}R^4+\mathcal{A}\left(13\sqrt{2}-8\sqrt{\mathcal{A}R^2+1}\sqrt{2\mathcal{A}R^2+1}\right)R^2\right.\\
&\left.+5\sqrt{2}-7\sqrt{\mathcal{A}R^2+1}\sqrt{2\mathcal{A}R^2+1}\right)\sqrt{\beta^2-3\beta+2}\Big]\chi_2\Big]\\
&\times\Big[\left(8\mathcal{A}^2\sqrt{2}R^4+\mathcal{A}\left(13\sqrt{2}-8\sqrt{\mathcal{A}R^2+1}\sqrt{2\mathcal{A}R^2+1}\right)R^2\right.\\
&\left.+5\sqrt{2}-7\sqrt{\mathcal{A}R^2+1}\sqrt{2\mathcal{A}R^2+1}\right)(\beta-1)\beta\Big(4\mathcal{A}^3\beta^2R^6\\
&+2\mathcal{A}^2\beta(3\beta+2)R^4+\mathcal{A}\left(3\beta^2+7\beta-2\right)R^2+4\beta\\
&+\left(8\mathcal{A}^3\beta^2R^6+2\mathcal{A}^2\beta(7\beta+4)R^4+\mathcal{A}\left(5\beta^2+17\beta-2\right)R^2\right.\\
&\left.+6\beta\right)\chi_2-2\Big)\Big]^{-1},
\end{aligned}
\tag{43}
$$

References

1. K. Schwarzschild, Math. Phys. 189–196 (1916)
2. K. Stelle, Phys. Rev. D **16**, 953–969 (1977)
3. S. Hawking, R. Penrose, Proc. R. Soc. Lond. **A314**, 529–548 (1970)
4. S. Weinberg, Rev. Mod. Phys. **61**, 1–23 (1989)
5. D. Lovelock, J. Math. Phys. **12**, 498–501 (1971)
6. T. Damour, G. Esposito-Farése, Class. Quantum Gravity **9**, 2093–2176 (1992)
7. G.W. Horndeski, Int. J. Theor. Phys. **10**, 363–384 (1974)
8. H.J. Schmidt, Int. J. Geom. Methods Mod. Phys. **4**, 209–248 (2007)
9. A. De Felice, S. Tsujikawa, Living Rev. Relativ. **13**, 3 (2010)
10. T. Clifton, P. Dunsby, R. Goswami, A.M. Nzioki, Phys. Rev. D **87**, 063517 (2013)
11. T. Clifton, P.K. Dunsby, Phys. Rev. D **91**, 103528 (2015)
12. J.T. Wheeler, Nucl. Phys. B **268**, 737 (1986)
13. I. Antoniadis, J. Rizos, K. Tamvakis, Nucl. Phys. B **415**, 497 (1994)
14. S. Nojiri, S.D. Odintsov, Phys. Lett. B **631**, 1 (2005)
15. A. De Felice, S. Tsujikawa, Phys. Lett. B **675**, 1 (2009)
16. R. Ferraro, F. Fiorini, Phys. Rev. D **75**, 084031 (2007)
17. R. Ferraro, F. Fiorini, Phys. Rev. D **78**, 124019 (2008)
18. G.R. Bengochea, R. Ferraro, Phys. Rev. D **79**, 124019 (2009)
19. G. Kofinas, E.N. Saridakis, Phys. Rev. D **90**(8), 084044 (2014)
20. T. Harko, F. Lobo, G. Otalora, E.N. Saridakis, JCAP **1412**, 021 (2014)
21. O. Bertolami, C.G. Boehmer, T. Harko, F. Lobo, Phys. Rev. D **75**, 104016 (2007)
22. T. Harko, Phys. Lett. B **669**, 376 (2008)
23. T. Harko, F. Lobo, Eur. Phys. J. C **70**, 373 (2010)
24. T. Harko, F. Lobo, S. Nojiri, S.D. Odintsov, Phys. Rev. D **84**, 024020 (2011)
25. M. Jamil, D. Momeni, M. Raza, R. Myrzakulov, Eur. Phys. J. C **72**, 1999 (2012)
26. M. Sharif, M. Zubair, JCAP **1203**, 028 (2012)
27. R. Myrzakulov, (2024). arXiv:1205.5266v8
28. M. Sharif, S. Rani, R. Myrzakulov, Eur. Phys. J. Plus **128**, 123 (2013)
29. R. Myrzakulov, L. Sebastiani, S. Zerbini, Int. J. Mod. Phys. D **22**, 1330017 (2013)
30. J.M. Nester, H.-J. Yo, Chin. J. Phys. **37**, 113 (1999)
31. B. Jimenez, L. Heisenberg, T. Koivisto, Phys. Rev. **98**, 044048 (2018)
32. A. Lymperis, JCAP **11**, 018 (2022)
33. B.C. Paul, A. Chanda, A. Beesham, S.D. Maharaj, Class. Quantum Gravity **39**(6), 065006 (2022)
34. S.A. Narawade, S.P. Singh, B. Mishra, Phys. Dark Univ. **42**, 101282 (2023)
35. O. Sokoliuk, S. Arora, S. Praharaj, A. Baransky, P.K. Sahoo, Mon. Not. R. Astron. Soc. **522**, 252–267 (2023)
36. M. Milgrom, Phys. Rev. D **100**(8), 084039 (2019)
37. F. D'Ambrosio, M. Garg, L. Heisenberg, Phys. Lett. B **811**, 135970 (2020)
38. F. Bajardi, D. Vernieri, S. Capozziello, Eur. Phys. J. Plus **135**, 912 (2020)
39. A.S. Agrawal, L. Pati, S.K. Tripathy, B. Mishra, Phys. Dark Univ. **33**, 100863 (2021)
40. G.N. Gadbail, A. Kolhatkar, S. Mandal, P.K. Sahoo, Eur. Phys. J. C **83**, 595 (2023)
41. N. Dimakis, A. Paliathanasis, T. Christodoulakis, Class. Quantum Gravity **38**, 225003 (2021)
42. F. Bajardi, S. Capozziello, Eur. Phys. J. C **83**, 531 (2023)
43. S.K. Maurya, K.N. Singh, M. Govender, G. Mustafa, S. Ray, Astrophys. J. Suppl. **269**(2), 35 (2023). https://doi.org/10.3847/1538-4365/ad0154
44. P. Bhar, K.N. Singh, S.K. Maurya, M. Govender, Phys. Dark Univ. **43**, 101391 (2024). https://doi.org/10.1016/j.dark.2023.101391
45. L. Heisenberg, Phys. Rep. **1066**, 1–78 (2024)
46. M.A. Alwan, T. Inagaki, B. Mishra, S.A. Narawade, JCAP **09**, 011 (2024). https://doi.org/10.1088/1475-7516/2024/09/011
47. F.G. Alvarenga, A. de la Cruz-Dombriz, M. Houndjo, M.E. Rodrigues, D. Saez-Gomez, Phys. Rev. D **87**, 103526 (2013)
48. V. Dzhunushaliev, V. Folomeev, B. Kleihaus, J. Kunz, Eur. Phys. J. C **74**, 2743 (2014)
49. T. Harko, Phys. Rev. D **90**, 044067 (2014)
50. V. Dzhunushaliev, V. Folomeev, B. Kleihaus, J. Kunz, Eur. Phys. J. C **75**, 157 (2015)
51. E.H. Baffou, M. Houndjo, M.E. Rodrigues, A.V. Kpadonou, J. Tossa, Phys. Rev. D **92**, 084043 (2015)
52. R.-J. Yang, Phys. Dark Univ. **13**, 87 (2016)
53. X. Liu, T. Harko, S.-D. Liang, Eur. Phys. J. C **76**, 420 (2016)
54. P. Moraes, J. Arbanil, M. Malheiro, JCAP **06**, 005 (2016)
55. M. Zubair, S. Waheed, Y. Ahmad, Eur. Phys. J. C **76**, 444 (2016)
56. M.-X. Xu, T. Harko, S.-D. Liang, Eur. Phys. J. C **76**, 449 (2016)
57. A. Salehi, S. Aftabi, JHEP **1609**, 140 (2016)
58. Z. Yousaf, M. Zaeem ul Haq Bhatti, Eur. Phys. J. C **76**, 267 (2016)
59. H. Shabani, A.H. Ziaie, Eur. Phys. J. C **77**, 31 (2017)
60. B.-M. Gu, Y.-P. Zhang, H. Yu, Y.-X. Liu, Eur. Phys. J. C **77**, 115 (2017)
61. M. Zubair, H. Azmat, I. Noureen, Eur. Phys. J. C **77**, 169 (2017)
62. M. Sharif, I. Nawazish, Eur. Phys. J. C **77**, 198 (2017)
63. E.H. Baffou, M. Houndjo, M. Hamani-Daouda, F.G. Alvarenga, Eur. Phys. J. C **77**, 708 (2017)
64. G.A. Carvalho, R.V. Lobato, P. Moraes, J. Arbanil, R.M. Marinho Jr., E. Otoniel, M. Malheiro, Eur. Phys. J. C **77**, 871 (2017)
65. P.K. Sahoo, P. Moraes, P. Sahoo, Eur. Phys. J. C **78**, 46 (2018)
66. P. Moraes, R. Correa, G. Ribeiro, Eur. Phys. J. C **78**, 192 (2018)
67. P.K. Sahoo, P. Sahoo, B.K. Bishi, S. Aygun, New Astron. **60**, 80 (2018)
68. H. Shabani, A.H. Ziaie, Int. J. Mod. Phys. A **33**, 1850050 (2018)

69. H. Shabani, A.H. Ziaie, Eur. Phys. J. C **78**, 397 (2018)
70. Z. Yousaf, M. Zaeem-ul-Haq Bhatti, M. Ilyas, Eur. Phys. J. C **78**, 307 (2018)
71. J. Wu, G. Li, T. Harko, S.-D. Liang, Eur. Phys. J. C **78**, 430 (2018)
72. T. Harko, F. Lobo, *Extensions of f(R) Gravity: Curvature-Matter Couplings and Hybrid Metric Palatini Theory* (Cambridge University Press, Cambridge, 2018)
73. Y. Xu, G. Li, T. Harko et al., f(Q, T) gravity. Eur. Phys. J. C **79**, 708 (2019)
74. A.S. Eddington, *Internal Constitution of the Stars* (Cambridge University Press, Cambridge, 1926)
75. N.K. Glendenning, *Compact Stars* (A&A Library, Springer, New York, 2000), p.82
76. E. Olson, M. Bailyn, Phys. Rev. D **12**, 3030 (1975)
77. E. Olson, M. Bailyn, Phys. Rev. D **13**, 2204 (1976)
78. H. Cuesta, A. Penna-Firme, A. P'erez-Lorenzana, Phys. Rev. D **67**, 087702 (2003)
79. J.A. de Diego, D. Dultzin-Hacyan, J.G. Trejo, D. Nunez, arXiv:astro-ph/0405237
80. V.F. Shvartsman, Sov. Phys. JETP **33**(3), 475 (1971)
81. S. Ray, A.L. Espindola, M. Malheiro, J. Lemos, V.T. Zanchin, Phys. Rev. D **68**, 084004 (2003)
82. M. Malheiro, R. Picanco, S. Ray, J. Lemos, V.T. Zanchin, Int. J. Mod. Phys. D **13**, 1375–79 (2004)
83. F. Weber, R. Negreiros, P. Rosenfield, *Neutron Stars and Pulsars, Astrophysics and Space Science Library*, vol. 357 (Springer, Berlin, 2009)
84. F. Weber, O. Hamil, K. Mimura, R.P. Negreiros, Int. J. Mod. Phys. D **19**, 1427–36 (2010)
85. B.V. Ivanov, Phys. Rev. D **65**, 104001 (2002)
86. R. Sharma, S. Mukherjee, S.D. Maharaj, Gen. Relativ. Gravit. **33**, 999 (2001)
87. M.K. Mak, T. Harko, Int. J. Mod. Phys. D **13**, 149 (2004)
88. K. Komathiraj, S.D. Maharaj, Gen. Relativ. Gravit. **39**, 2079 (2007)
89. S. Hansraj, S.D. Maharaj, Int. J. Mod. Phys. D **15**, 1311 (2006)
90. M.R. Finch, J. Skea, Class. Quantum Gravity **6**, 467 (1989)
91. Y. Xu et al., Eur. Phys. J. C **79**, 708 (2019)
92. J. Beltran Jimenez, L. Heisenberg, T. Koivisto, Phys. Rev. D **98**, 044048 (2018)
93. J. Beltran Jimenez, L. Heisenberg, T.S. Koivisto, S. Pekar, Phys. Rev. D **101**, 103507 (2020)
94. D. Zhao, Eur. Phys. J. C **82**, 303 (2022)
95. R.P. Negreiros, F. Weber, M. Malheiro, V. Usov, Phys. Rev. D **80**, 083006 (2009)
96. B.V. Ivanov, Int. J. Theor. Phys. **49**, 1236 (2010)
97. M.P. Korkina, O.Yu. Orlyanskii, Ukr. J. Phys. **36**, 885 (1991); translated to English from Ukr. Fiz. Zh. **36**(1), 127 (1991)
98. M.S.R. Delgaty, K. Lake, Comput. Phys. Commun. **115**, 395 (1998)
99. V. Varela, F. Rahaman, S. Ray, K. Chakraborty, M. Kalam, Phys. Rev. D **82**, 044052 (2010)
100. S.K. Maurya, Y.K. Gupta, S. Ray, S.R. Chowdhury, Eur. Phys. J. C **75**, 389 (2015)
101. S.K. Maurya, S. Ray, A. Aziz, M. Khlopov, P. Chardonnet, Int. J. Mod. Phys. D **28**, 1950053 (2019)
102. B. Dayanandan, T.T. Smitha, S.K. Maurya, Astrophys. Space Sci. **365**, 20 (2020)
103. F. de Felice, Y. Yu, J. Fang, Mon. Not. R. Astron. Soc. **277**, L17 (1995)
104. R. Ruderman, Rev. Astron. Astrophys. **10**, 427 (1972)
105. A. Errehymy et al., New Astron. **99**, 101957 (2023)
106. V. Canuto, in *Solvay Conf. on Astrophysics and Gravitation*, Brussels (1973)
107. L. Herrera, Phys. Lett. A **165**, 206 (1992)
108. S. Chandrashekhar, Phys. Rev. Lett. **12**, 114 (1964)
109. R.M. Wald, *General Relativity* (Chicago Press, Chicago and London, 1984), p.127
110. H. Bondi, Proc. R. Soc. Lond. Ser. A Math. Phys. Sci. **281**, 39 (1964)
111. M. Fortin, J.L. Zdunik, P. Haensel, M. Bejger, A&A **576**, A68 (2015)
112. F. Ozel, P. Freire, AR A&A **54**, 401 (2016)
113. E. Fonseca, H.T. Cromartie, T.T. Pennucci et al., APJL **915**, L12 (2021)
114. D. Kandel, R.W. Romani, ApJ **892**, 101 (2020)
115. P.V. Padmanabh et al., A&A **686**, A166 (2024)
116. R. Abbott, T.D. Abbott, S. Abraham et al., ApJL **896**, L44 (2020)
117. J.M. Lattimer, M. Prakash, ApJ **550**, 426 (2001)